Article

Seamless Signal Transduction from Three-Dimensional-Cultured Cells to a Superoxide Anions Biosensor via in Situ Self-Assembly of Dipeptide Hydrogel

Meiling Lian, Liang Xu, Xiaowen Zhu, Xu Chen, Wensheng Yang, and Tie Wang

Anal. Chem., **Just Accepted Manuscript** • DOI: 10.1021/acs.analchem.7b03371 • Publication Date (Web): 03 Nov 2017

Seamless Signal Transduction from Three-Dimensional-Cultured Cells to a Superoxide Anions Biosensor via in Situ Self-Assembly of Dipeptide Hydrogel

Meiling Lian,[†] Liang Xu,[†] Xiaowen Zhu,[†] Xu Chen,[*,†] Wensheng Yang,[†] and Tie Wang[*,‡,§]

[†]State Key Laboratory of Chemical Resource Engineering, Beijing University of Chemical Technology, Beijing 100029, China

[‡]Beijing National Laboratory for Molecular Sciences, Key Laboratory of Analytical Chemistry for Living Biosystems, Institute of Chemistry, Chinese Academy of Sciences, Beijing 100190, China

§University of Chinese Academy of Sciences, Beijing 100049, China

ABSTRACT: This study demonstrates a new strategy for the development of a three-dimensional (3D) cell culture model-based cellular biosensing system. Distinctly different from the previously reported layering or separating fabrication of cell culture and sensing devices, herein living cells and enzymes as sensing elements are immobilized into a dipeptide-derived hydrogel matrix through simple one-pot self-assembly. The cells are then 3D cultured in the functional hydrogel, and the releasing superoxide anion ($O_2^{\bullet-}$) is detected *in situ* by a cascade superoxide dismutase and horseradish peroxidase-based electrochemical biosensor. This novel design provides considerable advantages; including the possibility of capturing molecular signals immediately after they are secreted from living cells, due to the close proximity of the enzymes and the $O_2^{\bullet-}$-producing cells. Furthermore, incorporating all components in a 3D matrix provides a confinement environment, which can lead to concentrating effect of analysts. These properties allow the sensing device to achieve ultrahigh sensitivity and a precise response to a very low number of $O_2^{\bullet-}$ molecules. The proposed approach, based on the self-assembly of a small molecular hydrogel, also simplifies experimental procedures and increases protocol flexibility to cell culture methodology and sensing design. Consequently, this novel 3D culture model-based cellular biosensing system is envisaged to be useful for cellular function and pathology, drug discovery, and toxicity studies.

INTRODUCTION

Three-dimensional (3D) cell culture systems have attracted wide attention because of the wealth of physiologically relevant data and predictive information made available for *in vivo* testing.[1–3] The 3D structure not only influences the spatial organization of the cells, but also induces a physical constraint. These spatial and physical aspects affect the signal transduction from cells and ultimately influence cellular behaviors.[4] Accurate monitoring of the biological functions of 3D cultured cells requires detection and analysis of trace amounts of cell-secreted bio-interesting molecules.[5,6] Therefore, the development of an efficient sensing platform capable of sensitive, accurate, and stable monitoring of these molecules is needed to assess cell functionality and evaluate biological responses toward pharmaceutical compounds or toxic chemical species.[7,8] Considerable efforts have recently been devoted to construct various functional platforms.[9–11] However, the current strategies still require development for effective real-time detection of trace amount and short half-life substance (such as free radicals) released from 3D cultured cells. This is because raised diffusion distances in 3D culture models can cause significant recombination or degradation of the unstable molecules.[12,13] Since these molecules, e.g., reactive oxygen species (ROS), play a variety of roles in biological processes, such as signal transduction, inflammation, carcinogenesis, and neurodegenerative injury,[14] monitoring their release from 3D cultured cells is important but challenging.

To address the problem, it is crucial to develop an efficient strategy to quickly capture and sensitively detect these molecules when they are secreted.[15–22] Haruyama et al. assembled an organ-functional model on the surface of

* Address correspondence to chenxu@mail.buct.cn.
wangtie@iccas.ac.cn.

a nitric oxide (NO)-sensing matrix.[15] Notably, this construction decreased the distance between cells and sensors, thus the released NO was immediately trapped and tested. Tian et al. subsequently fabricated a dual-functional protein microarray for the selective culture of cells and detection of H_2O_2 released *in situ*.[16] Khademhosseini et al. constructed nanoporous gold for online monitoring of cellular superoxide anions ($O_2^{\bullet-}$).[17,18] Recently, our group developed a smart peptide-derived hydrogel biointerface for enzyme-based electrochemical biosensing, and cell adhesion and monitoring.[19] However, these works involved two-dimensional (2D) cell adhesion or culture. At this stage, the determination of ROS released from 3D cultured cells has rarely been reported. For the 3D cell culture-based detection platform, the following points must be taken into account. Firstly, the culture systems offer the possibility to better mimic the *in vivo* environment. The second aspect is related to established analysis methods, which must be adapted for application to 3D cell cultures and the corresponding platforms to fully capitalize on the advantages of 3D cell culture formats. The last is that the study of time-resolved responses of cell cultures upon application of a defined compound dosage often requires continuous read-out to ensure that important events are not missed.[5]

Inspired by research on self-assembled Fmoc dipeptide hydrogels for *in situ* 3D cell culture,[23] we demonstrate a novel strategy for constructing a cellular biosensing system for *in situ* measurement of superoxide anions ($O_2^{\bullet-}$) released from 3D cultured cells. The Fmoc dipeptide hydrogel was employed as both a 3D cell culture scaffold and an immobilized enzyme matrix. HeLa cells and two cascade enzymes, horseradish peroxidase (HRP) and superoxide dismutase (SOD), were simultaneously embedded inside the peptide hydrogel (hereafter CSH-hydrogel) by simple one-pot self-assembly (Scheme 1). Such an integrated design yielded considerable advantages for the determination of $O_2^{\bullet-}$, including a close proximity of recognized elements and cells, which can significantly minimize potential molecular decay. Therefore, the CSH-hydrogel platform ensures accurate and sensitive monitoring of $O_2^{\bullet-}$ released from the 3D cultured cells *in situ*.

EXPERIMENTAL SECTION

Chemicals and Solutions. Bachem (Bubendorf, Switzerland) provided N-Fluorenylmethoxycarbonyl diphenylalanine (Fmoc-FF). SOD (from bovine erythrocytes), 1,1,1,3,3,3-hexafluoro-2-propanol (HFIP), potassium superoxide (KO_2), and Zymosan A (Zym, from *Saccharomyces cerevisiae*) were purchased from Sigma-Aldrich. Shanghai Xueman Biotechnology Co. Ltd. (China) provided HRP (RZ ≥ 3, activity ≥ 250 units mg^{-1}). The $O_2^{\bullet-}$ solutions were obtained by adding the KO_2 powder to N_2-saturated phosphate-buffered saline (PBS) solution. The concentration of $O_2^{\bullet-}$ can be determined by recording the reduction of ferrocytochrome c using a spectrophotometer, and employing the extinction coefficient (21.1 mM^{-1} cm^{-1}) of ferrocytochrome c at 550 nm.[24]

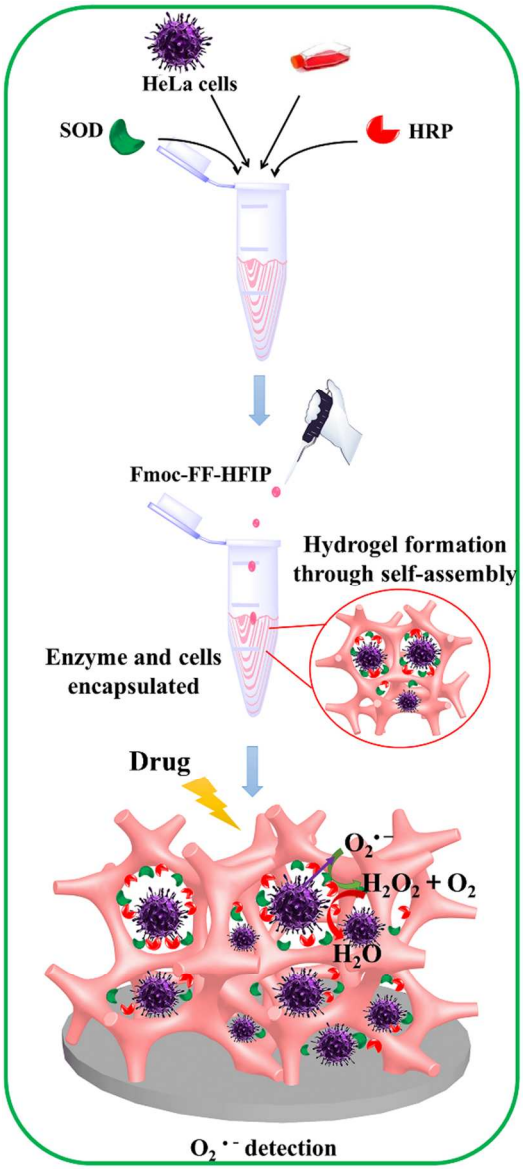

Scheme 1. Schematic illustration of the construction of a 3D cell culture-based electrochemical platform and its cell-monitoring assay.

Cell Culture and Preparation of the CSH-Hydrogel/GCE. HeLa cells were cultured in a humidified incubator (95% air with 5% CO_2) at 37°C in culture medium that was prepared by mixing sterile Dulbecco's Modified Eagle's Medium (DMEM), 1% penicillin, and 10% fetal bovine serum. The cells were harvested from the culturing petri dishes by trypsinization. The harvested cells were collected by centrifugation and suspended into the cell culture medium in different cell densities, such as 5.0×10^6 and 1.0×10^7 cells mL^{-1}.

Cell immobilization and 3D culture in the hydrogel were performed according to the following procedure. A

stock solution was freshly prepared by dissolving the lyophilized Fmoc-FF in HFIP at a concentration of 100 mg mL^{-1}, this mixture was then ultrasonicated until a clear solution was obtained. Subsequently, the stock solution was diluted with cell suspensions (5×10^6 cells mL^{-1}) containing 1 mg mL^{-1} HRP and 2000 U mL^{-1} SOD to reach the final concentration of 10 mg mL^{-1}. Figure S1 showed the photographs of the CSH-hydrogel within inverted vials. The concentrations of SOD and HRP in the hydrogel, as well as their ratios, were optimized according to analytical performance for $O_2^{\bullet-}$. The mixture solution (6 μL) was dropped on the surface of a clean glassy carbon electrode (GCE; 3 mm in diameter, pre-sterilized). The thickness of the formed hydrogel layer was approximately 49 μm, measured from the cross-sectional SEM images (Figure S2). The modified electrode was maintained in an incubator under a humidified atmosphere with 5% CO_2 at 37°C for 2 h to allow gelling and immobilization of the CSH-hydrogel on the surface of the GCE. The CSH-hydrogel/GCE was then immersed and suspended in culture medium. Using the Cell Counting Kit-8 (CCK-8, water-soluble tetrazolium salt) assay kit, cell proliferation was quantified; 1000 cells immobilized in the hydrogel containing dual-enzyme were plated into each well of a 96-well plate, in which 10 μL of CCK-8 was added to 100 μL of DMEM. The cells were subsequently incubated for 2 h at 37°C and the absorbance at 450 nm was measured with a microplate reader.

Other hydrogels incorporating partial components were prepared according to a similar procedure, and separately denoted as C-hydrogel (cells only), S-hydrogel (SOD only), H-hydrogel (HRP only), and SH-hydrogel (two enzymes).

In Situ Monitoring of $O_2^{\bullet-}$ Released from 3D Cultured Cells. The amperometric detection of $O_2^{\bullet-}$ released from 3D cultured cells was performed using the CSH-hydrogel/GCE as the working electrode. After reaching the steady-state current, 30 μg mL^{-1} Zym was added to the 0.1 M PBS solution (pH 7.0). The change in the current signal was monitored to indicate the amount of $O_2^{\bullet-}$ released from the 3D cultured HeLa cells. In addition, control experiments for the 2D cell culture method were also investigated. For mode 1, 6 μL of cell suspension (5×10^6 cells mL^{-1}) was dropped onto the SH-hydrogel/GCE. For mode 2, the SH-hydrogel/GCE was investigated by adding the same number of HeLa cells (3×10^4 cells) into the measured 0.1 M PBS solution (pH 7.0) (1 mL). The response change for $O_2^{\bullet-}$ released from cells was also recorded by adding the same amount of Zym into the 0.1 M PBS solution (pH 7.0).

Apparatus and Measurements. Scanning electron microscopy (SEM) images were taken by a Zeiss Supra 55 scanning electron microscope at an accelerating voltage of 20 kV. Fluorescence images were obtained using a confocal microscope (Leica TCS SP5). The UV–vis absorption spectra were obtained using a UV–vis spectrophotometer (PerkinElmer Lambda 35). Electrochemical measurements were performed on a CHI 660B electrochemical workstation (Shanghai CH Instruments, China). A conventional three-electrode system was used with a modified GCE as the working electrode, a platinum wire as the counter electrode and a saturated Ag/AgCl electrode as the reference electrode. The working solutions were purged with purified nitrogen for 20 min before testing, and a nitrogen atmosphere was maintained over the solutions during the electrochemical measurements.

RESULTS AND DISCUSSION

Ration Design of the CSH-Hydrogel. In this study, we chose Fmoc-FF derived hydrogel as a 3D cell culture matrix and biosensing platform because of its special features: (i) *In situ* formation makes the experimental design smart and flexible. It is feasible and facile to incorporate biomolecules including cells and sensing elements during the self-assembly process of Fmoc-FF.[19,23,25] After gelling, the immobilized cells can be 3D cultured *in situ* and recognized elements are uniformly distributed in the hydrogel. The close proximity between sensor and cells is thereby realized, which delivers considerably superior detection performance relative to the preassembly method[26] (detailed discussions seen supporting information). (ii) Furthermore, the gel is formed on or within an experimental structure, so the precursor can be dispensed into different kinds of patterned platforms such as lab-on-chips or microfluidic chips.[27,28] (iii) The π–π conjugation nanofiber structure of the hydrogel, derived from the self-assembly of Fmoc-FF, can facilitate electron transfer,[19] which is beneficial to the performance of electrochemical sensing.

To achieve the integration of 3D cell culture and sensor in the hydrogel, the following factors were considered for the design of the $O_2^{\bullet-}$ sensing system. Firstly, the sensing elements are satisfactorily biocompatible. After immobilization in the hydrogel, the cell viability is only slightly influenced or not at all. Secondly, the sensing performance in the hydrogel should be robust. Since enzymes are inherent to organisms and immobilization in hydrogel matrices may result in the improvement of their activity and stability in the complex environment,[29,30] an enzyme-based electrochemical biosensing system is appropriate for the present design. SOD is effective and most frequently used for $O_2^{\bullet-}$ sensing.[31–34] Thus, the electrochemical behavior of SOD immobilized in the Fmoc peptide hydrogel was explored. Nevertheless, direct electron transfers between SOD and the GCE were not realized (Figure S3). In our previous study,[19] HRP encapsulated within the hydrogel matrix showed direct electrochemistry behavior and good sensing performance for H_2O_2. Therefore, SOD and HRP bi-enzymes were employed in this work for sensing of $O_2^{\bullet-}$ based on a well-known cascade reaction mechanism (Scheme 1). It is noted that the bi-enzyme detection design inevitably results in interference from cascade HRP substrate (herein H_2O_2). An improved design will be explored in future work.

Characterization of the CSH-Hydrogel. The hydrogel samples with and without biomolecules were prepared by adding a stock Fmoc-FF agent into purified water or cell suspension solution of both enzymes, followed by self-assembly of the mixture solution and gelling at moderate temperature. The SEM images in Figure S2 revealed that the hydrogels with enzymes had porous 3D networks, which consisted of numerous nanofibers with diameters of approximately 30–40 nm. Confocal microscopy was employed to confirm whether HRP and SOD were embedded in the hydrogel. Initially, the amino group of enzymes was conjugated with fluorescein isothiocyanate (FITC), which was used as the fluorescent label. As shown in the fluorescent image (Figure 1A), it can be clearly seen that the enzymes were uniformly incorporated in the hydrogel and mainly distributed along the nanofibers. No fluorescence was observed for the bare gel, indicating that the fluorescent image observed in Figure 1A is ascribed to the two enzymes immobilized in the hydrogel. To further demonstrate that SOD and HRP were successfully encapsulated in the hydrogel, element mapping was performed. It can be seen that the Fe (characteristic element of HRP), Cu, and Zn (characteristic elements of SOD) were uniformly distributed through both hydrogels, indicating the successful encapsulation of HRP and SOD in the SH-hydrogel (Figure S4). These results validated the suggestion that both SOD and HRP could be conveniently and uniformly incorporated into the hydrogel by a self-assembly process. Additionally, the leakage of the dual enzymes after being immobilized in the hydrogel was investigated (seen in the supporting information). The results indicated that most HRP and SOD were stably entrapped within the network of the hydrogel, which is supported by a previous study reporting that molecules larger than 5 kDa were firmly immobilized in the peptide hydrogel.[25] Note that the molecular weight of HRP, SOD, and cells are much higher than 5 kDa. Therefore, the Fmoc-FF hydrogel can be used efficiently for enzyme and cell encapsulation. The activity of the dual enzymes was also evaluated. As shown in the Figure S5A, the peak located at 403 nm, corresponding to the Soret band of the heme protein in the UV-vis absorption spectrum for SH-hydrogel, was not changed relative to solution-state HRP. This implies that HRP maintained its basic secondary structure and processed its intrinsic activity.[35] The SOD enzyme within the hydrogel retained 74% of its activity relative to the free enzymes, based on the ability of SOD to inhibit the autoxidation of pyrogallol (Figure S5B).[36] The relatively high activities of HRP and SOD within the hydrogel make it a potential effective platform for cell monitoring.

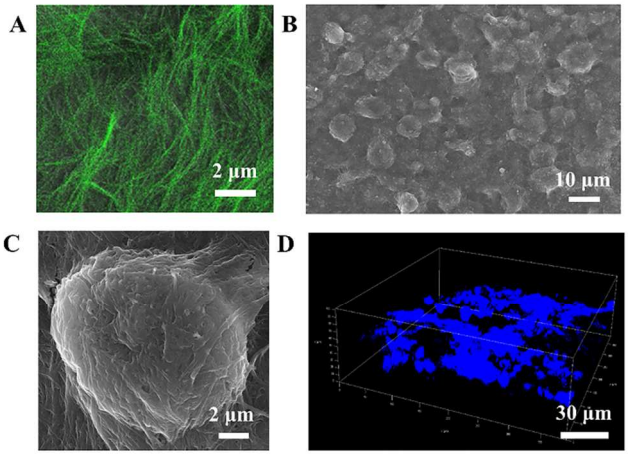

Figure 1. (A) Confocal microscopic image of SH-hydrogel, (B) scanning electron microscopy image, (C) a high-magnification view, (D) three-dimensional (3D) view of laser scanning confocal microscopy z-stacks of the CSH-hydrogel.

Figure 1B shows a typical SEM of the CSH-hydrogel with HeLa cells. It can be clearly seen that a number of rounded cells with a diameter of 10 μm are embedded throughout the gel matrix. The cells are wrapped in nanofibers, as depicted in the enlarged SEM image (Figure 1C). To aid visualization of the hydrogel matrix, cells were stained with Hoechst 33342, which revealed that cells suspended in the hydrogel sample tend to adopt a 3D structure in the 3D view of laser scanning confocal microscopy z-stack images (Figure 1D), rather than the elongated conformation in surface cultures. The support provided by a 3D gel results in more spherical cell growth. This arrangement more closely models the *in vivo* growth of cells seen in tissues, which may have significant implications in cell studies as more relevant and realistic results are desired.[23] Furthermore, cell proliferation was determined by a CCK-8 assay (Figure S6). Relatively little growth was detected, while cell viability remained over the first three days, which is similar to previously observed phenomena.[23]

Analytical Properties of the CSH-Hydrogel-Based Cellular Biosensor. The CSH-hydrogel/GCE as the working electrode was connected to a computerized electrochemical analyzer with a three-electrode system for further electrochemical biosensing of $O_2^{\bullet-}$. Cyclic voltammetry was first employed to study the electrochemical behavior of the modified electrodes. Figure 2A depicts the cyclic voltammograms of different modified electrodes in both the presence and absence of 100 nM $O_2^{\bullet-}$. A pair of well-defined redox peaks at –0.327 and –0.276 V was obtained at the CSH-hydrogel/GCE (curve a in Figure 2A), while only charge currents were observed at the modified electrodes without HRP in the hydrogel (Figure S1). This suggests that the redox peak originated from the oxidation and reduction of the active Fe(III)/Fe(II) center of

HRP.[37,38] Furthermore, the formal potential and the peak-to-peak separation of the CSH-hydrogel/GCE are closely similar to the values for the H-hydrogel/GCE, implying that the introduction of cells and SOD to hydrogel did not obviously influence the direct electron transfer between HRP and the electrodes. After the addition of 100 nM $O_2^{\bullet-}$, a significant increase in cathodic peak current and an accompanied decrease of the anodic peak current were observed at the CSH-hydrogel/GCE, while the CH-hydrogel/GCE without SOD did not show a similar change. This demonstrates that the increasing response for $O_2^{\bullet-}$ was attributed to the cascade reaction mechanism (Figure 2B): The $O_2^{\bullet-}$ can be converted to H_2O_2 and molecular oxygen by catalysis of SOD, and subsequently generated H_2O_2 is converted to water and molecular oxygen by HRP, meanwhile electrocatalytic reduction currents are recorded at the modified electrode. The effect of different scan rates on the electrochemical response of the CSH-hydrogel were also studied. As shown in Fig. S7, the cathodic peak currents increase linearly with the scan rate (υ), which implies that the electrode reaction is a surface-controlled redox process.[39]

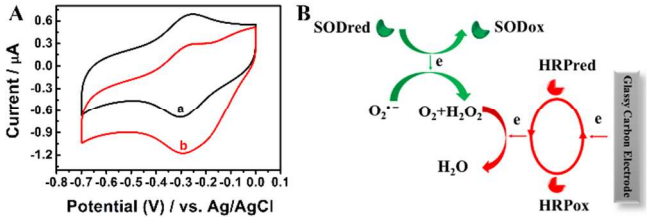

Figure 2. (A) Cyclic voltammograms of CSH-hydrogel/glassy carbon electrode (GCE) with (a) 0 and (b) 100 nM $O_2^{\bullet-}$ in 0.1 M phosphate-buffered saline (PBS) solution (pH 7.0) at a scan rate of 0.1 V s^{-1}. (B) Scheme of the mechanism of sensing hydrogel to $O_2^{\bullet-}$.

Amperometry was used to investigate the response of the CSH-hydrogel/GCE to continuous addition of $O_2^{\bullet-}$ into N_2-saturated 0.1 M PBS solution at –0.35 V. As shown in Figure 3A, a stepwise current response with increasing $O_2^{\bullet-}$ concentration was observed at the sensor, reaching 95% of the steady-state current less than 5 s. The corresponding calibration curve is presented in Figure 3B. A linear response range was acquired from 0.96 to 187.62 nM with a correlation coefficient of 0.998. The biosensor exhibited a low detection limit of 0.34 nM based on a signal-to-noise ratio (S/N) of 3 and a high sensitivity of 85.02 μA μM^{-1} cm^{-2}. Compared with other modified electrodes (Table S1), our proposed sensor exhibited much higher sensitivity and a lower detection limit. The sensitive response of the CSH-hydrogel/GCE was mainly attributed to two aspects; the Fmoc peptide hydrogel provides a biocompatible environment for immobilized enzymes, which ensures the maintenance of enzyme activity. Furthermore, bi-enzymes immobilized in the hydrogel network could result in a confinement effect, which may reduce the diffusion distance and concentrate the products. This may greatly improve the sensitivity of the sensor.

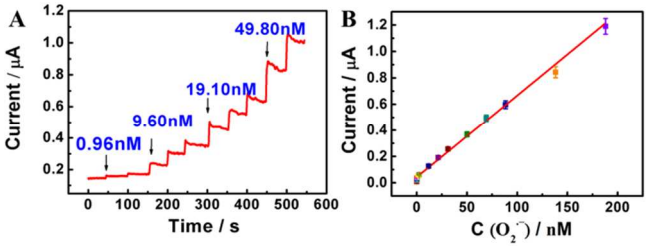

Figure 3. (A) Current-time response of the CSH-hydrogel/GCE to the continuous addition of $O_2^{\bullet-}$ in stirred 0.1 M PBS solution (pH 7.0) at –0.35 V. (B) Plot of steady-state current vs. $O_2^{\bullet-}$ concentration.

In addition, the analytical performance of a control-modified electrode without cultured cells in the hydrogel (SH-hydrogel/GCE) was also examined under the same conditions (Figure S8A). A linear relationship was observed in concentration ranges of $O_2^{\bullet-}$ from 1.05 to 242.31 nM (Figure S8B). The detection limit was estimated to be 0.35 nM (S/N = 3) with a sensitivity of 95.28 μA μM^{-1} cm^{-2} for the linear ranges. The difference between these results and those obtained at the CSH-hydrogel/GCE is not obvious. This property is very crucial to the construction of *in situ* 3D cell culture-based cellar sensing devices,[17] as it may reduce the calibration times of the sensors based on different culture days and increase the reproducibility of the sensors.

The selectivity of the biosensor for $O_2^{\bullet-}$ was investigated by adding interfering substances; for instance, dopamine, ascorbic acid, uric acid, tyrosine, citric acid, glucose, Ca^{2+}, Mg^{2+}, Ni^{2+}, and Ag^{+}. No obvious amperometric responses were observed at –0.35 V, suggesting that the presence of these species did not affect the detection of $O_2^{\bullet-}$ (Figure S9A). However, 100 nM H_2O_2 produced 28% of the cathodic current response relative to 100 nM $O_2^{\bullet-}$. This is reasonable, because the sequential enzyme biosensor was fabricated with SOD and HRP. In addition, when the CSH-hydrogel/GCE was stored at 37°C in the medium and used for the detection of 100 nM $O_2^{\bullet-}$, the response of the current maintained more than 89% of its original value in 7 days (Figure S9B). Moreover, for five determinations using an electrode, the relative standard deviation (RSD) was 3.2%. Five CSH-hydrogel/GCEs prepared independently were used to test 100 nM $O_2^{\bullet-}$, and collectively yielded a RSD of 6.8%. Thus, the stability and reproducibility of the current biosensor was satisfactory.

***In situ* Monitoring of 3D Cellular $O_2^{\bullet-}$ Production.** The constructed CSH-hydrogel/GCE was further applied to *in situ* monitoring of $O_2^{\bullet-}$ released from 3D cultured HeLa cells in the hydrogel. Zym was chosen as the functional drug to stimulate living cells to release molecular $O_2^{\bullet-}$.[40,41] The dynamic response of HeLa cells seeded at a density of 5.0×10^6 cells mL^{-1} after 2 days of culture are presented in Figure 4A and D. As soon as 30 μg mL^{-1} Zym

was added into the PBS solution, a significant current response (about 103.9 nA) appeared. In the control experiment, the SH-hydrogel/GCE without HeLa cells showed negligible current increase after injecting the same amount of Zym. Furthermore, when the seeded cell density increased to 1.0 × 10^7 cells mL^{-1}, the current response also increased to 192.4 nA (Figure S10). In addition, the responses of the CSH-hydrogel/GCE for different culture days were measured, as shown in Figure S11. The amounts of released $O_2^{\bullet-}$ slowly increased within 5 days, which is possibly attributed to the small amount of cell proliferation. The influence of Zym concentration on the release of $O_2^{\bullet-}$ was also researched. The current response of $O_2^{\bullet-}$ increased with the increase of the concentration of Zym, as shown in Figure S12. This indicated that the observed signal was dependent on Zym concentration.

Based on the drug-stimulated current response (103.9 nA) and the data regarding the $O_2^{\bullet-}$ sensor performance (Figure 3B), the released $O_2^{\bullet-}$ concentration was roughly estimated to be 9.64 nM. This value is larger than those obtained from previously reported conventional procedures,[24,42,43] in which living cells directly adhered to the modified electrode[42] (Figure 4B, E) and the $O_2^{\bullet-}$ sensor electrode was physically located near living cell lines in solution[24,43] (Figure 4C, F). These quantitative results suggest that the $O_2^{\bullet-}$ concentration was very high in the vicinity of the cell surface. It is well understood that a portion of $O_2^{\bullet-}$ is inevitably recombined or degraded during the diffusion process between sensor and cells in the separated fabrication.[17,45] In our design, the produced $O_2^{\bullet-}$ is immediately captured by the surrounding enzymes, and the signal transduction can be effectively monitored by the modified electrode. All processing was finished within the CSH-hydrogel matrix. In addition, it is also noted that the lifetime of the released $O_2^{\bullet-}$ in the present 3D model is longer than those obtained from control experiments in 2D cell culture modes (both in solution and adhered to the electrode surface) (Figure 4). This unique hydrogel provides a 3D restricted space, resulting in the concentrating effect of $O_2^{\bullet-}$, and therefore increase the lifetime of the released $O_2^{\bullet-}$. Consequently, the proposed design is promising for studying the dynamics of the generation and demise of $O_2^{\bullet-}$ under physiological conditions, and exploring the role and mechanism of $O_2^{\bullet-}$ in activities *in vivo*.[44,45]

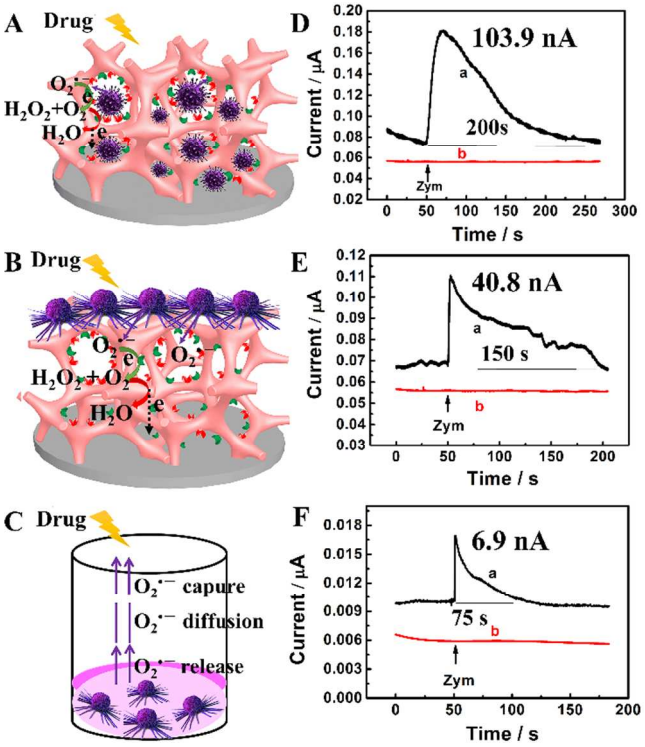

Figure 4. Scheme showing the path of $O_2^{\bullet-}$ detection in cells (A) cultured in the SH-hydrogel (3D cell culture), (B) adhered on SH-hydrogel/GCE (mode 1 of 2D cell culture), and (C) grown in a culture dish (mode 2 of 2D cell culture). Amperometric responses of SH-hydrogel/GCE under cells with (D) 3D cell culture mode, (E) mode 1 of 2D cell culture, and (F) mode 2 of 2D cell culture in the presence (a) and absence (b) of HeLa cells (3 × 10^4 cells) induced by Zym (30 μg mL^{-1}) in 0.1 M PBS (pH 7.0) at –0.35 V vs. Ag/AgCl.

CONCLUSIONS

In general, we have validated a new strategy for the technically simple preparation of a 3D culture model-based cellular biosensing system through rational design and one-step self-assembly of an Fmoc peptide hydrogel. The efficient integration of HeLa cells and bi-enzymes into the matrix allowed for the immediate capture and sensitive detection of released $O_2^{\bullet-}$. The proposed CSH-hydrogel-based biosensor exhibits a superior sensitivity of 85 μA μM^{-1} cm^{-2} and a low detection limit of 0.34 nM for $O_2^{\bullet-}$. Quantitative determination of $O_2^{\bullet-}$ released from *in situ* 3D cultured cells in the hydrogel has been successfully illustrated. Compared to other assays for detecting $O_2^{\bullet-}$ released by cells, this integrated platform delivers several key advantages: a close proximity of enzymes and $O_2^{\bullet-}$-producing cells with an extremely short diffusion distance endows an ultrahigh sensitivity to the sensor. Also, the 3D restricted of hydrogel and concentrating effect of $O_2^{\bullet-}$ gives the $O_2^{\bullet-}$ a longer dead time. 3D models that can precisely recapitulate the important architecture and func-

tionality of their in vivo counterparts than conventional 2D surface growth, provides more accurate and predictive data. Since the self-assembled process of the hydrogel is convenient for the incorporation of various sensing elements, such as recognized peptides, this work yielded promising results for the monitoring of some bio-interesting molecules secreted from 3D cultured cells, especially for highly unstable and easily decayed substrates. Therefore, this study is envisaged to be of great importance in both understanding the behavior and function of cells *in vivo* and testing drug efficacy and toxicity *in vitro*.

ASSOCIATED CONTENT

Supporting Information

Comparison of performances from $O_2^{\bullet-}$ biosensors, photograph, AFM image and SEM of CSH-hydrogel, CVs of different electrodes and scan rates, activity of HRP and SOD, cell proliferation assay, selectivity and stability experiments, and current responses at different amount of cells, different days and different concentration of Zym are shown in the Supporting Information. This material is available free of charge via the Internet at http://pubs.acs.org.

AUTHOR INFORMATION

Corresponding Author

E-mail: chenxu@mail.buct.edu.cn. Phone: +86-10-64435271.
Email: wangtie@iccas.ac.cn. Phone: +86-10-82362042.

Corresponding Author

Xu Chen: 0000-0001-6187389
Tie Wang: 0000-0001-5965-6520

Notes

The authors declare no competing financial interest.

ACKNOWLEDGMENT

This work was supported by the National Natural Science Foundation of China (21521005, 21656001, 21321003, 21635002, 21422507) and Beijing Engineering Center for Hierarchical Catalysts.

REFERENCES

(1) Rodenhizer, D.; Gaude, E.; Cojocari, D.; Mahadevan, R.; Frezza, C.; Wouters, B. G.; McGuigan, A. P. *Nat. Mater.* **2016**, *15*, 227–234.

(2) Feiner, R.; Engel, L.; Fleischer, S.; Malki, M.; Gal, I.; Shapira, A.; Diamand Y. S.; Dvir, T. *Nat. Mater.* **2016**, *15*, 679–685.

(3) Shamir, E. R.; Ewald, A. J. *Nat. Rev. Mol. Cell Biol.* **2014**, *15*, 647–664.

(4) Yang, L.; Trivedi, G.; Adcock, A. F.; Tyson, W. *ECS Trans.* **2014**, *64*, 125–132.

(5) Misun, P. M.; Rothe, J.; Schmid, Y. R.; Hierlemann, A.; Frey, O. *Microsyst. Nanoeng.* **2016**, *2*, 16022.

(6) Zhang, Y. S.; Aleman, J.; Shin, S. R.; Kilic, T.; Kim, D.; Shaegh, S. A. M.; Massa S.; Riahi R.; Chae S.; Hu N.; Avci H.; Zhang W.; Silvestri A.; Nezhad A.S.; Manbohi A.; Ferrari F. D.; Polini A.; Calzone G.; Shaikh N.; Alerasool P.; Budina E.; Kang J.; BHISE N.; Ribas J.; Pourmand A.; Skardal A.; Shupe T.; Bishop C. E.; Dokmeci M.R.; Atala A.; Khademhosseini A. *P. Natl. Acad. Sci. USA* **2017**, *114*, 2293–2302.

(7) Choi, J.; Lee, E. K.; Choo, J.; Yuh, J.; Hong, J. W. *Biotechnol. J.* **2015**, *10*, 1682–1688.

(8) Shin, S. R.; Kilic, T.; Zhang, Y. S.; Avci, H.; Hu, N.; Kim, D.; Branco C.; Aleman J.; Massa S.; Silvestri A.; Kang, J.; Desalvo A.; Hussaini M. A.; Chae S.; Polini A.; Bhise N.; Hussain M. A.; Lee H.Y.; Dokmeci M. R.; Khademhosseini A. *Adv. Sci.* **2017**, *4*, 1600522.

(9) Abe, H.; Ino, K.; Li, C. Z.; Kanno, Y.; Inoue, K. Y.; Suda, A.; Kunikata R.; Matsudarira M.; Takahashi Y.; Shiku H.; Matsue, T. *Anal. Chem.* **2015**, *87*, 6364–6370.

(10) Shin, S. R.; Zhang, Y. S.; Kim, D. J.; Manbohi, A.; Avci, H.; Silvestri, A.; Aleman J.; Hu N.; Kilic T.; Keung W.; Righi M.; Assawes P.; Alhadrami H. A.; Li R. A.; Dokmeci M. R.; Khadehosseini A. *Anal. Chem.* **2016**, *88*, 10019–10027.

(11) Weltin, A.; Hammer, S.; Noor, F.; Kaminski, Y.; Kieninger, J.; Urban, G. A. *Biosens. Bioelectron.* **2017**, *87*, 941–948.

(12) Freeman, B. A.; Crapo, J. D. *Lab. Invest.* **1982**, *47*, 412–426.

(13) Batchelor, A. M.; Bartus, K.; Reynell, C.; Constantinou, S.; Halvey, E. J.; Held, K. F.; Held K. F.; Dostmann W.R.; Vernon J.; Garthwaite, J. *P. Natl. Acad. Sci. USA* **2010**, *107*, 22060–22065.

(14) Chen, X.; Wang, F.; Hyun, J. Y.; Wei, T.; Qiang, J.; Ren, X.; Shin I.; Yoon, J. *Chem. Soc. Rev.* **2016**, *45*, 2976–3016.

(15) Asakawa, H.; Mochitate, K.; Haruyama, T. *Anal. Chem.* **2008**, *80*, 1505–1511.

(16) Li, X.; Liu, Y.; Zhu, A.; Luo, Y.; Deng, Z.; Tian, Y. *Anal. Chem.* **2010**, *82*, 6512–6518.

(17) Sadeghian, R. B.; Ostrovidov, S.; Han, J.; Salehi, S.; Bahraminejad, B.; Bae, H.; Chen M.; Khademhosseini, A. *ACS Sens.* **2016**, *1*, 921–928.

(18) Sadeghian, R. B.; Han, J.; Ostrovidov, S.; Salehi, S.; Bahraminejad, B.; Ahadian, S.; Chen M.; Khademhosseini, A. *Biosens. Bioelectron.* **2017**, *88*, 41–47.

(19) Lian, M.; Chen, X.; Lu, Y.; Yang, W. *ACS Appl. Mater. Interfaces* **2016**, *8*, 25036–25042.

(20) Liu, Y. L.; Wang, X. Y.; Xu, J. Q.; Xiao, C.; Liu, Y. H.; Zhang, X. W.; Liu J.T.; Huang, W. H. *Chem. Sci.* **2015**, *6*, 1853–1858.

(21) Liu, Y. L.; Jin, Z. H.; Liu, Y. H.; Hu, X. B.; Qin, Y.; Xu, J. Q.; Xu J.Q.; Fan C.F.; Huang, W. H. *Angew. Chem.* **2016**, *128*, 4613–4617.

(22) Hu, F. X.; Kang, Y. J.; Du, F.; Zhu, L.; Xue, Y. H.; Chen, T.; Dai L. M.; Li, C. M. *Adv. Funct. Mater.* **2015**, *25*, 5924–5932.

(23) Liebmann, T.; Rydholm, S.; Akpe, V.; Brismar, H. *BMC biotechnol.* **2007**, *7*, 88.

(24) Ma, X.; Hu, W.; Guo, C.; Yu, L.; Gao, L.; Xie, J.; Li, C. M. *Adv. Funct. Mater.* **2014**, *24*, 5897–5903.

(25) Kim, J. H.; Lim, S. Y.; Nam, D. H.; Ryu, J.; Ku, S. H.; Park, C. B. *Biosens. Bioelectron.* **2011**, *26*, 1860–1865.

(26) Jayawarna, V.; Ali, M.; Jowitt, T. A.; Miller, A. F.; Saiani, A.; Gough, J. E.; Ulijn, R. V. *Adv. Mater.* **2006**,*18*, 611–614.

(27) Lakshmanan, A.; Zhang, S.; Hauser, C. A. *Trends Biotechnol.* **2012**, *30*, 155–165.

(28) Wei, G.; Su, Z.; Reynolds, N. P.; Arosio, P.; Hamley, I. W.; Gazit, E.; Mezzenga, R. *Chem. Soc. Rev.* **2017**, *46*, 4661–4708.

(29) Zhai, D.; Liu, B.; Shi, Y.; Pan, L.; Wang, Y.; Li, W.; Zhang R.; Yu, G. *ACS Nano* **2013**, *7*, 3540–3546.

(30) Li, L.; Wang, Y.; Pan, L.; Shi, Y.; Cheng, W.; Shi, Y.; Yu, G. *Nano lett* **2015**, *15*, 1146–1151.

(31) Tian, Y.; Mao, L.; Okajima, T.; Ohsaka, T. *Anal. Chem.* **2004**, *76*, 4162–4168.

(32) Li, X. R.; Wang, B.; Xu, J. J.; Chen, H. Y. *Nanoscale* **2011**, *3*, 5026–5033.

(33) Zhu, X.; Niu, X.; Zhao, H.; Tang, J.; Lan, M. *Biosens. Bioelectron.* **2015**, *67*, 79–85.

(34) Zhu, X.; Liu, T.; Zhao, H.; Shi, L.; Li, X.; Lan, M. *Biosens. Bioelectron.* **2016**, *79*, 449–456.

(35) Xie, Q.; Zhao, Y.; Chen, X.; Liu, H.; Evans, D. G.; Yang, W. *Biomaterials* **2011**, *32*, 6588–6594.

(36) Wang, X.; Niu, D.; Li, P.; Wu, Q.; Bo, X.; Liu, B.; Bao S.; Su T.; Xu H.; Wang, Q. *ACS Nano*, **2015**, *9*, 5646–5656.

(37) Liu, H. H.; Tian, Z. Q.; Lu, Z. X.; Zhang, Z. L.; Zhang, M.; Pang, D. W. *Biosens. Bioelectron.* **2004**, *20*, 294–304.

(38) Lavanya, N.; Radhakrishnan, S.; Sekar, C. *Biosens. Bioelectron.* **2012**, *36*, 41–47.

(39) Wang, Y.; Wang, Z.; Rui, Y.; Li, M. *Biosens. Bioelectron.* **2015**, *64*, 57–62.

(40) Lin, Q. Y.; Jin, L. J.; Cao, Z. H.; Lu, Y. N.; Xue, H. Y.; Xu, Y. P. *Phytother. Res*. **2008**, *22*, 740–745.

(41) Wang, M. Q.; Ye, C.; Bao, S. J.; Zhang, Y.; Xu, M. W.; Li, Z. *Chem. Commun.* **2016**, *52*, 12442–12445.

(42) Yuan, L.; Liu, S.; Tu, W.; Zhang, Z.; Bao, J.; Dai, Z. *Anal. Chem.* **2014**, *86*, 4783-4790.

(43) Shen, X.; Wang, Q.; Liu, Y.; Xue, W.; Ma, L.; Feng, S.; Wan M.; Wang F.; Mao, C. *Sci. Rep.* **2016**, *6*, 28989.

(44) Hartmann, P.; Grübl, D.; Sommer, H.; Janek, J.; Bessler, W. G.; Adelhelm, P. *J. Phys. Chem. C* **2014**, *118*, 1461–1471.

(45) Hansel, C. M., Buchwald, C., Diaz, J. M., Ossolinski, J. E., Dyhrman, S. T., Van Mooy, B. A. S., Polyviou, D. *Limnol. Oceanogr.* **2016**, *61*, 1188–1200.

Table of contents